J Therm Anal Calorim (2012) 107:345–354
DOI 10.1007/s10973-011-1434-8

Thermal decomposition kinetics of tetraalkylammonium and dimethylpyridinium salts of the complex anion bis(1,3-dithiole-2-thione-4,5-dithiolate) bismuthate (−1)

Ana Maria Rocco · James L. Wardell · Robson Pacheco Pereira

Received: 9 December 2010 / Accepted: 23 February 2011 / Published online: 10 March 2011

Abstract In the present work, thermal decomposition kinetics of tetraalkylammonium and 1,4-dimethylpyridinium salts of the complex anion bis(1,3-dithiole-2-thione-4,5-dithiolate) bismuthate ($[Bi(dmit)_2]^-$) are addressed. Kinetic parameters for the decomposition reactions were obtained utilizing the Ozawa and Coats–Redfern (CR) models. Entropy, enthalpy, and free energy of decomposition processes were calculated from the CR results, providing information on the thermodynamic characteristics of the processes. The most probable mechanisms of thermal decomposition were indicated for the studied systems, along with their kinetic and thermodynamic parameters.

Keywords Kinetics · dmit · Complexes

Introduction

In the last two decades, there has been a great interest in metal complexes, organometallics and related molecular conductive systems due to the possibility of obtaining new materials with optimized properties for technological applications [1, 2]. The metal-like conductivity and superconductivity are among the most interesting phenomena observed in these materials. In the late 1980s, Kobayashi [3] described the structure of the salt $[NMe_4]_{0.5}[Ni(dmit)_2]$, ($NMe_4$ = tetramethyl ammonium and dmit = 1,3-dithiole-2-thione-4,5-dithiolate, Fig. 1), where layers of parallel planar units of $[Ni(dmit)_2]$ exist in the periodic structure, generating a π electron delocalization on the solid. Until now, many publications have addressed these systems and much effort is pointed to their synthesis and crystal structure determination.

The solid-state structures of various salts of dmit-based anions contain sulfur bridge interactions, resulting in extended (or polymeric) structures, which, associated to the pseudo-aromatic behavior of the π electrons of the ring, make these materials suitable for technological applications which require fine control of small electronic currents [4]. Applications based on organometallic ferromagnets, non-linear optical materials, and conducting polymers are the main focus of research in this area since the 1990s [5, 6].

Salts of dmit complex anions can also be used as precursors of thin films, for which physicochemical solid-state characterization and knowledge of the kinetic parameters involved in thermal decomposition are necessary. Among the methods for obtaining thin solid films, thermal decomposition of precursors is an alternative, easier and less expensive process than are chemical vapor deposition [7] or Languimuir–Blodgett techniques [8]. In addition, hybrid films of conducting polymers and dmit complexes exhibit enhanced electrical and electrochemical properties [9] and, due to the possible applications of these materials in electronic devices, understanding their decomposition kinetics is a key issue.

Among these metal–dmit complexes, $[Zn(dmit)_2]^{2-}$ salts have a particular role as stable dmit precursor for use

A. M. Rocco (✉)
Grupo de Materiais Condutores e Energia, Escola de Química, Universidade Federal do Rio de Janeiro, Cidade Universitária, Rio de Janeiro 21941-909, Brazil
e-mail: amrocco@eq.ufrj.br

J. L. Wardell
Fundacao Oswaldo Cruz FIOCRUZ, CDTS, Rio de Janeiro 21040900, Brazil

R. P. Pereira
Instituto de Ciências Exatas (ICEx), Universidade Federal Fluminense, Volta Redonda, RJ 27213-415, Brazil

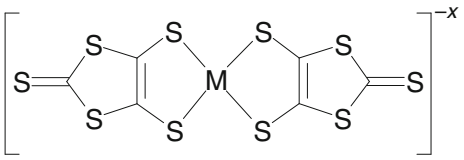

Fig. 1 Schematic molecular structure of $[M(dmit)_2]^{-x}$ anions

with other metals. Some structures of dmit complexes with Zn, $[Q]_2[Zn(dmit)_2]$ (Q = monovalent cation), have been reported [10]; these complexes exhibit different tendencies to associate in the solid state via S…S contacts [11]. In $[Q]_2[Zn(dmit)_2]$, the metal atoms are solely bonded to the dithiolate sulfur atoms within the anions, and thus have distorted tetrahedral geometries. Particularly for [Q][Bi(dmit)$_2$], the packing of the anions in solid state is strongly dependent on $[Q^+]$ [12].

The main goal of the present work is to study the thermal decomposition kinetics of tetraalkylammonium and dimethylpyridinium salts of bis(1,3-dithiole-2-thione-4,5-dithiolate) bismuthate (−1) and to determine the most probable mechanisms for the solid-state reactions involved, correlating them with the crystalline structures and the cations in [Q][Bi(dmit)$_2$].

Methods

The decomposition process under non-isothermal conditions can be studied from a single thermogravimetric (TG) curve utilizing the Achar differential equation [13], the MacCallum–Tanner method [14], the Horowitz–Metzger approximation method [15], or the Coats–Redfern (CR) integral equation [16]. The Ozawa equation [17] can also be used to obtain kinetic parameters associated with a non-isothermal decomposition process, in which several different heating rates are used.

In the present work, the CR (Eq. 1) and Ozawa (Eq. 2) methods were utilized to study the thermal decomposition processes. The models and functions for the most common mechanisms operating in solid-state decompositions, which have been tested in the present work, are well known and can be found in the literature.

$$\ln\left[\frac{g(\alpha)}{T^2}\right] = \ln\left[\frac{AR}{\phi E_a}\left(1-\frac{2RT}{E_a}\right)\right] - \frac{E_a}{RT} \quad (1)$$

$$\log\phi + \frac{0.4567E_a}{RT} = C \quad (2)$$

In the above equations, α is the fractional decomposition, T is the absolute temperature (K), A is the pre-exponential Arrhenius factor (s^{-1}), ϕ is the heating rate (K s^{-1}), E_a is the apparent activation energy (J mol^{-1}), R is the gas constant (J mol^{-1} K^{-1}), $g(\alpha)$ is the integral function, and C is a constant value. For the CR equation, $2RT/E_a \ll 1$ and the plot of $\ln[g(\alpha)/T^2]$ versus $1/T$ would give a straight line [18]. E_a is then calculated from the slope and A was obtained from the intercept.

Utilizing the data obtained from the CR equation, the activation entropy ($\Delta S^{\#}$), activation enthalpy ($\Delta H^{\#}$), and free energy of activation ($\Delta G^{\#}$) were calculated as follows [19]:

$$\Delta S^{\#} = 2.303\log\left(\log\frac{Ah}{kT_m}\right)R \quad (3)$$

$$\Delta H^{\#} = E_a - RT_m \quad (4)$$

$$\Delta G^{\#} = \Delta H^{\#} - T_m\Delta S^{\#}, \quad (5)$$

where h and k are the Planck and Boltzmann constants, respectively, and T_m is the peak temperature of the DTG curve.

Experimental

The salts [1,4-dimethyl pyridinium][Bi(dmit)$_2$], [Me_2Py][Bi(dmit)$_2$] (I), [NBu_4][Bi(dmit)$_2$] (II), and [NEt_4][Bi(dmit)$_2$] (III) were synthesized and characterized previously by our group and the results can be found in details in the references [13]. [Me_2Py]Br, [NBu_4]Br, and [NEt_4]Br were purchased from Aldrich Chemical Co., stored under dry argon atmosphere and used without further purification. A Perkin-Elmer TGA7 system was used for the TG analysis and the experiments were carried out under a nitrogen atmosphere from room temperature to 600 °C with heating rates of 5, 10, 15, and 20 K min^{-1}. The flow rate of nitrogen was maintained constant at 50 cm^3 min^{-1}. The initial mass of finely powdered samples was kept about 4 mg. Superficial conductivity measures were carried out utilizing a nanovoltimeter HP and a four-probe electrode system. Samples of the salts I, II, and III, previously synthesized and characterized [8, 16], were submitted to 6 ton pressure in order to obtain homogeneous pellets for the superficial conductivity measures in a dry box.

Results and discussion

Superficial conductivity

The superficial conductivity values measured in a dry box under argon atmosphere with humidity <0.01 ppm for the samples I, II, and III, are ($1.13 \pm 0.18 \times 10^{-7}$), ($1.65 \pm 0.09 \times 10^{-3}$), and ($2.50 \pm 0.23 \times 10^{-6}$) Ω^{-1} cm^{-1}, respectively. The values obtained show a variation, of about four orders of magnitude, depending on the cation.

This behavior has already been described for other complex systems [3] and it is known that the structural changes induced by cation exchange strongly affect the electrical properties of such systems [4]. For the studied compounds, different crystal structures may be formed depending on the cation, which reflects on the electrical properties of the solids.

Thermal stability

TG curves at heating rates of 5, 10, 15, and 20 K min^{-1} for the salts I, II, and III are shown in Figs. 2, 3, and 4, respectively. All three complex salts exhibited multi-step decomposition processes: the temperature and mass loss data for the [Q][Bi(dmit)$_2$] and [Q]Br salts are listed in Table 1, where the temperature ranges are defined from the onset temperature (start of the decomposition at the lower heating rate) to the endset temperature (end of the decomposition at the higher heating rate), covering the entire range of decomposition temperatures for each step studied. Despite the fact that systems I, II, and III exhibit multi-step thermal decomposition curves, only III presents superimposable TG curves, which do not (strongly) change their shape for different heating rates. This characteristic allows the calculation of the kinetic parameters by the Ozawa method for the consecutive decomposition steps. For salts I and II, only the first decomposition step on the curve does not change with the heating rate and, consequently, only this step was analyzed by the Ozawa method. The first decomposition step of I begins at 180 °C, while decompositions for II and III begin at approximately 170 °C (both recorded at heating rates of 5 K min^{-1}). The first decomposition step of I occurs between 180 and 225 °C with 18% mass loss, and that of II, in the range of

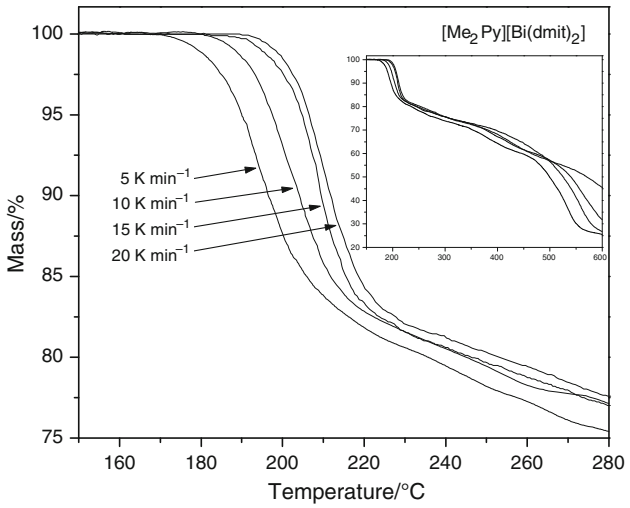

Fig. 2 TG curves for [Me_2Py][Bi(dmit)$_2$]

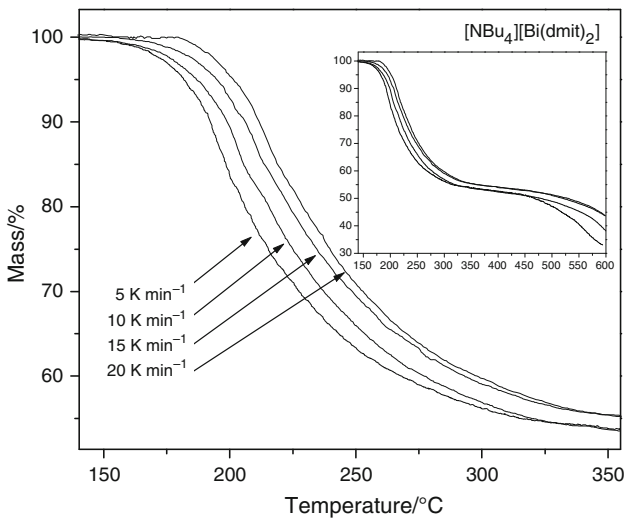

Fig. 3 TG curves for [NBu_4][Bi(dmit)$_2$]

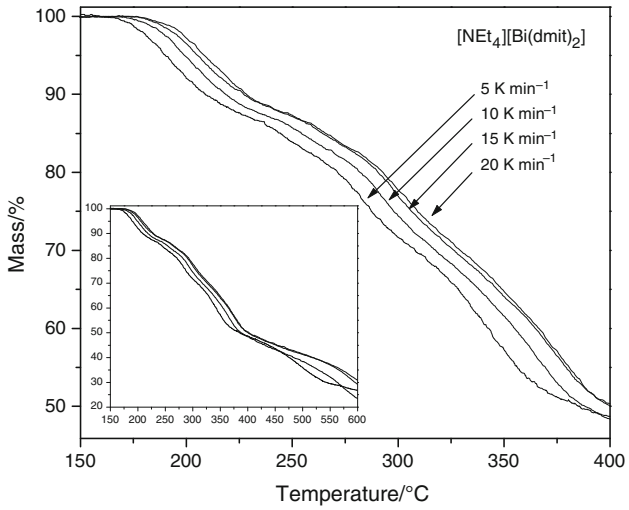

Fig. 4 TG curves for [NEt_4][Bi(dmit)$_2$]

Table 1 Temperature and mass loss data for [Q][Bi(dmit)$_2$] and [Q]Br salts

	Compound	Temperature decomposition range/°C	Mass loss/%
I	[Me_2Py][Bi(dmit)$_2$]	180–225	18
	[Me_2Py]Br	160–260	100
II	[NBu_4][Bi(dmit)$_2$]	170–320	45
	[NBu_4]Br	155–211	100
III	[NEt_4][Bi(dmit)$_2$]		
	First step	170–245	15
	Second step	260–330	40
	Third step	335–390	20
	[NEt_4]Br	225–270	100

170–320 °C with a mass loss of 45%. These mass loss values do not change with the heating rate, which enables the analysis of these decomposition steps by the Ozawa method. In Fig. 4, it can be seen that the decomposition of III occurs in three consecutive steps, the first in the temperature range of 170–245 °C, with mass loss of 15%; the second from 260 to 330 °C, with mass loss of 40% and the third in the range of 335–390 °C. A similar multi-step thermal decomposition was observed for a Co-dmit complex by Melo and co-workers [20]. In Melo's paper, the decomposition kinetics was studied utilizing the Zaskó method and the decomposition of the complex occurred in two consecutive steps. The first occurred step at approximately 170 °C, similar to the temperature observed for the decompositions of II and III. The Zaskó method, however, does not provide information about the mechanism of the thermal decomposition. In the present work, as well as the kinetics study, the most probable mechanisms for the thermal decompositions are also described.

The bromide salts of the cations, [Q]Br, were studied in order to detect the influence of the cation, Q^+, on the thermal decomposition of the [Q][Bi(dmit)$_2$] salts. The TG curves for [Me_2Py]Br, [NBu_4]Br, and [NEt_4]Br are shown in Figs. 5, 6, and 7, respectively. For all the [Q]Br salts, thermal decompositions occur in a single step leading to the complete decomposition of the sample. The decomposition of tetraalkylammonuim and 1,4-dimethylpyridinium bromides has not been reported previously in the literature up to our knowledge and, comparing the [Q]Br TG curves with those for [Q][Bi(dmit)$_2$], there seems to be no obvious relationship between the nature of the cation and the onset temperature for the decomposition of [Q][Bi(dmit)$_2$]. As mentioned, the onset of the thermal decomposition for II and III is about 170 °C, while exchanging tetraalkylammonium by 1,4-dimethylpyridinium, the onset shifts to 180 °C.

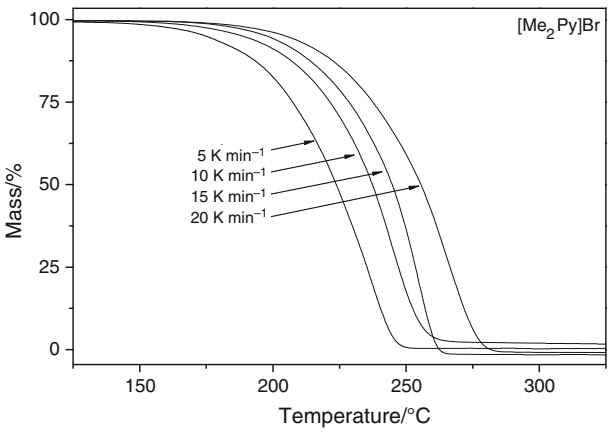

Fig. 5 TG curves for [Me_2Py]Br

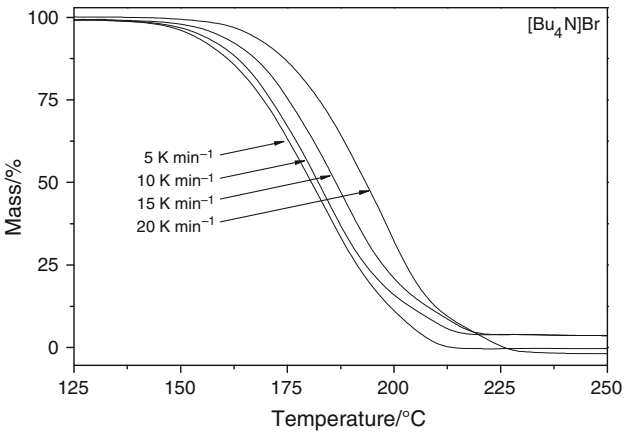

Fig. 6 TG curves for [NBu_4]Br

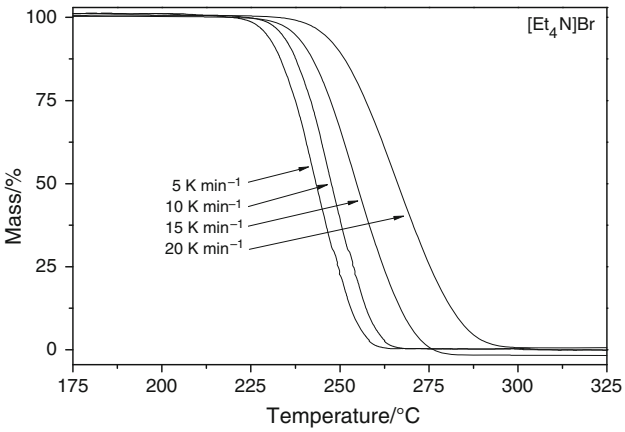

Fig. 7 TG curves for [NEt_4]Br

Kinetic parameters

In order to apply the Ozawa method [17] to study the kinetics of a particular decomposition process, the thermal decomposition curves must shift in the abscissa when the heating rate is changed, however, the mass loss and the difference between $T_{(endset)}$ and $T_{(onset)}$ must not change with heating rate. For each I and II, only the first step in the thermal decomposition behaves as assumed in the Ozawa method. For all systems, however, the CR method was applied.

Despite the assumptions and general considerations of Ozawa and CR methods are different, the combined information acquired from the application of both to complex systems may result in a more detailed description. Recently, the CR method has been used successfully to describe the thermal decomposition kinetics of different systems [21, 22].

Table 2 lists the values of E_a, log(A), r (correlation coefficient), $\Delta S^{\#}$, $\Delta H^{\#}$, and $\Delta G^{\#}$, for the first step of decomposition of compounds I, II, and III and the second and third steps of III utilizing the CR method. The

Table 2 Kinetic parameters, correlation coefficients (r), and thermodynamic functions for I, II, and III calculated utilizing the CR method (heating rate 5 K min^{-1})

	Mechanism	E_a/kJ mol^{-1}	log (A)	r	$\Delta S^{\#}$/J mol^{-1}	$\Delta H^{\#}$/kJ mol^{-1}	$\Delta G^{\#}$/kJ mol^{-1}
I							
$Me_2Py[Bi(dmit)_2]$	$*D_1$	552.49	58.33	0.99270	868.01	548.54	135.66
	$*D_2$	581.74	61.34	0.99436	925.65	577.79	137.50
	$*D_3$	584.19	60.97	0.99443	918.56	580.24	143.32
	$*D_4$	582.56	60.78	0.99438	914.92	578.61	143.42
	$*F_1$	289.42	30.70	0.99435	338.98	285.47	124.23
	F_2	26.79	0.96	0.95079	−230.46	22.84	132.45
	F_3	54.33	3.43	0.94108	−183.16	50.38	137.50
	P_3	130.52	13.60	0.99069	11.56	126.57	121.07
	$A_{1.5}$	179.67	18.90	0.99173	113.04	175.72	121.95
	A_2	132.79	13.86	0.99148	16.54	128.84	120.97
	A_3	85.91	8.77	0.99094	−80.92	81.96	120.44
	A_4	62.47	6.19	0.99035	−130.32	58.52	120.50
	R_2	271.15	28.32	0.99161	293.41	267.20	127.64
	R_3	271.91	28.23	0.99173	291.69	267.96	129.22
II							
$[NBu_4][Bi(dmit)_2]$	$*D_1$	240.09	24.42	0.99474	218.02	235.78	122.81
	$*D_2$	241.74	24.32	0.9951	216.11	237.43	125.46
	$*D_3$	243.42	23.87	0.99544	207.49	239.11	131.60
	$*D_4$	242.30	23.73	0.99521	204.81	237.99	131.87
	$*F_1$	118.74	11.93	0.99544	−21.12	114.43	125.38
	F_2	3.54	−1,12	0.98343	−270.99	−0.77	139.65
	F_3	12.46	0.46	0.98635	−240.74	8.15	132.89
	P_3	52.36	4.80	0.99045	−157.64	48.05	129.74
	$A_{1.5}$	68.29	6.46	0.98592	−125.86	63.98	129.20
	A_2	49.27	4.42	0.98465	−164.92	44.96	130.42
	A_3	30.26	2.32	0.98162	−205.13	25.95	132.24
	A_4	20.75	1.21	0.97770	−226.38	16.44	133.74
	R_2	107.49	10.29	0.98943	−52.53	103.18	130.40
	R_3	108.04	10.18	0.98979	−54.63	103.73	132.04
III							
$[NEt_4][Bi(dmit)_2]$	$*D_1$	38.70	1.62	0.99936	−217.91	34.70	139.44
First step of dec.	$*D_2$	42.81	1.77	0.99903	−215.03	38.81	142.17
	$*D_3$	47.29	1.60	0.99885	−218.29	43.29	148.21
	$*D_4$	44.31	1.27	0.99906	−224.61	40.31	148.27
	$*F_1$	20.69	0.37	0.99733	−241.84	16.69	132.93
	F_2	11.70	−0.33	0.95136	−255.24	7.70	130.39
	F_3	4.54	−0.79	0.98711	−264.05	0.54	127.46
	P_3	1.94	−2.10	0.98778	−289.13	−2.06	136.92
	$A_{1.5}$	10.29	−0.69	0.99612	−262.14	6.29	132.29
	A_2	5.17	−1.36	0.99152	−274.97	1.17	133.34
	A_3	-2.25×10^{-2}	–	0.84835	–	–	–
	A_4	−2.61	–	0.99502	–	−6.61	–
	$*R_2$	17.41	−0.33	0.99845	−255.24	13.41	136.10
	$*R_3$	18.47	−0.37	0.99829	−256.01	14.47	137.53

Table 2 continued

	Mechanism	E_a/kJ mol^{-1}	log (A)	r	$\Delta S^{\#}$/J mol^{-1}	$\Delta H^{\#}$/kJ mol^{-1}	$\Delta G^{\#}$/kJ mol^{-1}
Second step of dec.	$*D_1$	46.51	2.36	0.99331	−205.13	41.79	158.33
	$*D_2$	46.84	2.12	0.99186	−209.72	42.12	161.27
	$*D_3$	46.55	1.46	0.99231	−222.36	41.83	168.16
	$*D_4$	47.66	1.56	0.99155	−220.45	42.94	168.18
	F_1	19.55	0.21	0.98866	−246.30	14.83	154.76
	F_2	7.30	−0.66	0.97666	−262.95	2.58	151.97
	F_3	16.10	0.63	0.97441	−238.25	11.38	146.74
	P_3	4.77	−1.47	0.96254	−278.46	0.05	158.25
	$A_{1.5}$	11.42	−0.55	0.98073	−260.85	6.70	154.90
	A_2	6.73	−1.11	0.97140	−271.57	2.01	156.30
	A_3	−0.17	–	0.92874	–	−4.89	–
	A_4	−2.17	–	0.98052	–	−6.89	–
	R_2	19.59	−0.11	0.98719	−252.42	14.87	158.28
	R_3	20.65	−0.15	0.98743	−253.19	15.93	159.78
Third step of dec.	D_1	403.30	42.15	0.98111	555.80	398.02	44.72
	D_2	352.55	35.99	0.97202	437.86	347.27	68.94
	D_3	353.71	35.47	0.97239	427.90	348.43	76.43
	D_4	352.94	35.38	0.97215	426.18	347.66	76.76
	$*F_1$	173.55	17.77	0.99151	89.00	168.27	111.70
	F_2	9.30	−0.40	0.97510	−258.91	4.02	168.59
	F_3	15.66	0.58	0.97517	−240.14	10.38	163.02
	P_3	86.30	8.61	0.97202	−86.39	81.02	135.93
	$A_{1.5}$	120.59	12.30	0.97537	−15.74	115.31	125.31
	A_2	88.51	8.88	0.97427	−81.22	83.23	134.85
	A_3	56.43	5.39	0.97186	−148.05	51.15	145.25
	A_4	40.39	3.60	0.96910	−182.32	35.11	151.00
	R_2	183.93	18.68	0.97595	106.42	178.65	111.00
	R_3	184.20	18.53	0.9761	103.55	178.92	113.10

mechanisms that give the best correlation coefficients are marked with an asterisk. For the third decomposition step of salt III, the values of r indicate that the mechanism of the thermal decomposition is F_1, with $E_a \sim 173.55$ kJ mol^{-1} and log(A) $\sim$ 17.77, calculated using the CR method. Considering the F_1 mechanism, $\Delta S^{\#}$, $\Delta H^{\#}$, and $\Delta G^{\#}$ values for this step were 89.00 J mol^{-1}, 168.27 kJ mol^{-1}, and 111.70 kJ mol^{-1}, respectively. For the first and second steps of decomposition of salt III, however, more than one mechanism results in good correlation coefficients and it is not possible to choose among them based only on the results of the CR method. For both I and II, the mechanisms D_1, D_2, D_3, D_4, and F_1 showed a good agreement with the experimental data, however, the values of r (correlation coefficients) do not allow the unambiguously identification of the mechanism for the thermal decomposition of these salts. Sánchez and co-workers [23], studying pentamethylcyclopentadienylrhodium (II) complexes, pointed out that identification of the mechanism was not possible utilizing only the values of the correlation coefficients from the CR or MacCallum–Tanner methods. Different approaches have been made for the supplementary analysis of the kinetic data, based both on TG or DTG (first derivative of TG curve) curve shape. The method proposed by Dollimore [24, 25] allows one to separate mechanisms into groups. In the present work, this approach is used in combination with the Ozawa and CR methods in order to distinguish among the possible mechanisms of thermal decomposition.

It is important to determine the kinetics of decomposition of [Me_2Py]Br, [NBu_4]Br, and [NEt_4]Br and to compare these with those of the equivalent [Q][Bi(dmit)$_2$] complexes in order to identify the influence of the cation on the decomposition of systems I, II, or III. The values of E_a, log(A), r, $\Delta S^{\#}$, $\Delta H^{\#}$, and $\Delta G^{\#}$ obtained for [Q]Br, utilizing the CR method are listed in Table 2 and the functions that give the better correlation coefficients are marked with an asterisk. In Table 3, the kinetic parameters and correlation coefficients for [Q]Br, calculated utilizing the CR method,

are listed. The correlation coefficients obtained for [Me_2Py]Br (D_n, $n = 1$–3; P_3) [NBu_4]Br (D_n, $n = 1$ or 3; P_3; A_n, $n = 2$ or 4; R_2) and [NEt_4]Br (F_1; $A_{1.5}$, A_2) exhibits differences only in the third decimal place and do not allow the unambiguous identification of the thermal decomposition mechanism for these salts.

Table 3 Kinetic parameters, correlation coefficients (r), and thermodynamic functions for [Q]Br calculated utilizing the CR method (heating rate 5 K min^{-1})

	Mechanism	E_a/kJ mol^{-1}	log (A)	r	$\Delta S^{\#}$/J mol^{-1}	$\Delta H^{\#}$/kJ mol^{-1}	$\Delta G^{\#}$/kJ mol^{-1}
[Me_2Py]Br	$*D_1$	193.55	19.07	0.99957	116.17	189.53	133.41
	$*D_2$	202.54	19.81	0.99974	130.34	198.52	135.55
	$*D_3$	213.24	20.39	0.99777	141.44	209.22	140.89
	D_4	204.92	19.44	0.99931	123.25	200.90	141.35
	F_1	108.29	10.70	0.99262	−44.09	104.27	125.58
	F_2	632.64	64.10	0.88312	978.36	628.62	155.93
	F_3	1274.05	128.76	0.88445	2216.42	1270.03	199.17
	$*P_3$	42.58	3.61	0.99914	−179.85	38.56	125.46
	$A_{1.5}$	68.90	6.55	0.99222	−123.55	64.88	124.58
	A_2	49.45	4.46	0.99165	−163.57	45.43	124.46
	A_3	30.75	2.39	0.99032	−203.21	26.73	124.91
	A_4	21.06	1.25	0.98869	−225.03	17.04	125.77
	R_2	99.11	9.32	0.99889	−70.52	95.09	129.16
	R_3	101.47	9.43	0.99764	−68.41	97.45	130.51
[NBu_4]Br	$*D_1$	238.34	26.73	0.99351	263.31	234.55	114.44
	D_2	231.29	25.59	0.99029	241.48	227.50	117.34
	$*D_3$	245.18	26.67	0.99369	262.16	241.39	121.80
	D_4	235.87	25.51	0.99156	239.95	232.08	122.62
	F_1	119.95	13.38	0.99254	7.70	116.16	112.65
	F_2	103.67	12.10	0.98178	−16.81	99.88	107.55
	F_3	215.11	25.46	0.98295	239.00	211.32	102.30
	$*P_3$	57.31	6.06	0.99508	−132.46	53.52	113.94
	$A_{1.5}$	80.11	8.78	0.99366	−80.38	76.32	112.98
	$*A_2$	59.08	6.30	0.99354	−127.86	55.29	113.61
	A_3	36.42	3.55	0.99164	−180.52	32.63	114.97
	$*A_4$	27.91	2.51	0.99665	−200.43	24.12	115.54
	$*R_2$	121.69	13.27	0.99408	5.59	117.90	115.35
	R_3	118.74	12.74	0.99247	−4.56	114.95	117.03
[NEt_4]Br	D_1	483.74	47.64	0.98864	662.58	479.41	134.44
	D_2	458.57	44.73	0.98018	606.86	454.24	138.28
	D_3	497.11	48.08	0.98931	671.00	492.78	143.42
	D_4	471.35	45.40	0.98205	619.69	467.02	144.38
	$*F_1$	269.75	26.70	0.99498	261.64	265.42	129.20
	F_2	313.57	31.74	0.90086	358.14	309.24	122.78
	F_3	586.05	59.53	0.87477	890.24	581.72	118.22
	P_3	126.27	12.26	0.99026	−14.85	121.94	129.67
	$*A_{1.5}$	175.78	17.29	0.99502	81.46	171.45	129.04
	$*A_2$	129.97	12.67	0.99481	−7.00	125.64	129.28
	A_3	84.28	8.00	0.99401	−96.41	79.95	130.15
	A_4	61.11	5.59	0.99316	−142.56	56.78	131.00
	R_2	235.11	22.78	0.98318	186.58	230.78	133.64
	R_3	244.20	23.56	0.98911	201.52	239.87	134.95

Table 4 Characterization of the mechanisms based on the shape of TG plots and the values of $\Delta LoT/\Delta HiT$

	System	Characteristics of $T_{(onset)}$ and $T_{(endset)}$	$\Delta LoT/\Delta HiT$	Associated mechanisms
I	$[Me_2Py][Bi(dmit)_2]$	$T_{(onset)}$ d; $T_{(endset)}$ d	1.02	F_n ($n = 1, 2, 3$)
	$[Me_2Py]Br$	$T_{(onset)}$ d; $T_{(endset)}$ s	3.57	R_n ($n = 2, 3$); D_n ($n = 1, 2, 3, 4$)
II	$[NBu_4][Bi(dmit)_2]$	$T_{(onset)}$ d; $T_{(endset)}$ d	0.96	F_n ($n = 1, 2, 3$)
	$[NBu_4]Br$	$T_{(onset)}$ d; $T_{(endset)}$ d	1.21	F_n ($n = 1, 2, 3$)
III	$[NEt_4][Bi(dmit)_2]$			
	First step	$T_{(onset)}$ d; $T_{(endset)}$ d	0.99	F_n ($n = 1, 2, 3$)
	Second step	$T_{(onset)}$ d; $T_{(endset)}$ d	1.01	F_n ($n = 1, 2, 3$)
	Third step	$T_{(onset)}$ d; $T_{(endset)}$ d	0.97	F_n ($n = 1, 2, 3$)
	$[NEt_4]Br$	$T_{(onset)}$ s; $T_{(endset)}$ s	0.94	A_n ($n = 2, 3, 4$)

d diffuse, *s* sharp

Table 5 Values of the apparent activation energy and correlation coefficients (r) calculated for all the studied systems utilizing the Ozawa method

System	E_a/kJ mol^{-1}	r
$[Me_2Py][Bi(dmit)_2]$	294.4	0.9867
$[Me_2Py]Br$	185.2	0.9911
$[NBu_4][Bi(dmit)_2]$	110.2	0.9952
$[NBu_4]Br$	137.6	0.9975
$[NEt_4][Bi(dmit)_2]$		
First step	61.1	0.9964
Second step	70.6	0.9974
Third step	164.8	0.9991
$[NEt_4]Br$	126.5	0.9908

Using the approach of Dollimore and co-workers [24], the ΔLoT and ΔHiT parameters (which are the low and high temperature fractions of the DTG half-width peak) were determined from the DTG curves for the different systems. In Table 4, the values of $\Delta LoT/\Delta HiT$ and the characteristics of $T_{(onset)}$ and $T_{(endset)}$ with the associated mechanisms are shown. From the analysis of the data in Table 4, there is an indication that the salts I, II, III and $[NBu_4]Br$ exhibit decomposition processes governed by the F_n mechanisms, $[Me_2Py]Br$ by R_n or D_n, and $[NEt_4]Br$, by A_n. A separation by the parameters listed in Table 4 enables the mechanism to be identified or, at worst, narrows the choice down to a few mechanisms [24]. In the present case, the possible mechanisms were grouped, and the comparison of the data obtained with the other methods (CR and Ozawa) allows the determination of the most probable mechanisms.

The apparent activation energy of the decomposition processes was calculated using the Ozawa equation, in which four different heating rates were used. The calculated values of E_a and r are shown in Table 5. The analyses of the data in Table 5 showed that, despite the fact that Ozawa method neglects the mechanism function in calculating kinetic parameters [17], the apparent activation energy values are in good agreement with some of those found utilizing the CR method. The comparison of the E_a values obtained from the Ozawa and CR equations, combined with the analysis of the TG–DTG curve, allows one to distinguish among the different possible mechanisms. This approach was utilized by Diefallah in the study of the kinetics of the non-isothermal decomposition of manganese acetate tetrahydrate [26].

Based on the different analyses carried out, the most probable mechanisms of thermal decomposition are listed in Table 6. The decomposition of salts I, II and the third decomposition step of III may be associated with a process involving the anion $[Bi(dmit)_2]^-$, since all the mechanisms determined are F_1 (first order), independent of the cation. For the [Q]Br salts, there are different probable mechanisms, indicating that both the cation and solid-state structures strongly influence the kinetics of thermal decomposition. The analysis of the mechanisms also indicates that the cation is not involved in the first step of decomposition of $[Q][Bi(dmit)_2]$ salts.

The crystalline structures of I and II are comparable and the interactions between the ligands and the bismuth atom are similar. The structure of III, however, is quite unique, exhibiting the dmit as a bridging ligand, which results in strong intermolecular interactions than formed in the structures of I and II. The differences in the crystal structures account for the higher decomposition temperature of compound III.

Considering the most probable decomposition mechanism for each salt, as listed in Table 6, activation entropy values tend to be positive, except for $[NBu_4][Bi(dmit)_2]$ and $[NEt_4]Br$. This general behavior reflects a higher

Table 6 Most probable mechanisms for the decomposition of each salt and summary of the kinetic and thermodynamic parameters (determined using the CR method)

Compound	Most probable mechanism	Decomposition function	E_a/kJ mol^{-1}	log (A)	$\Delta S^{\#}$/J mol^{-1}	$\Delta H^{\#}$/kJ mol^{-1}	$\Delta G^{\#}$/kJ mol^{-1}
$[Me_2Py][Bi(dmit)_2]$	F_1	$-\ln(1-\alpha)$	289.42	30.70	338.98	285.47	124.23
$[Me_2Py]Br$	D_1	α^2	193.55	19.07	116.17	189.53	133.41
$[NBu_4][Bi(dmit)_2]$	F_1	$-\ln(1-\alpha)$	118.74	11.93	−21.12	114.43	125.38
$[NBu_4]Br$	R_2	$1-(1-\alpha)^{1/2}$	121.69	13.27	5.59	117.90	115.35
$[NEt_4][Bi(dmit)_2]$							
First step	D_n	–	–	–	–	–	–
Second step	D_n	–	–	–	–	–	–
Third step	F_1	$-\ln(1-\alpha)$	173.55	17.77	89.00	168.27	111.70
$[NEt_4]Br$	A_2	$[-\ln(1-\alpha)]^{1/2}$	129.97	12.67	−7.00	125.64	129.28

disorder of the products in comparison with the reactants, since most of these products may be eliminated in the gas phase. Other complex systems with similar structure around the central metal ion (a distorted octahedron) exhibit a similar behavior, such as the complex of manganese(II) with 1-phenyl-3-methyl-4-benzoyl-5-pyrazolone [27]. While there are differences in the entropy values, activation enthalpy values are positive for all systems and activation free energy values are found in a narrow range between 111.70 and 133.41 kJ mol^{-1}.

The $\Delta H^{\#}$ positive values obtained for the decomposition reactions reflect the endothermic characteristic of the processes, while the positive values of $\Delta G^{\#}$ are associated with the non-spontaneity of the reactions, which is observed for the decomposition of other inorganic systems [28].

Conclusions

Thermal decomposition of bismuth–dmit complex salts was studied by non-isothermal kinetics, using Ozawa and CR methods. These methods allowed to obtain the most probable mechanisms for these systems, the kinetic and thermodynamic parameters associated with the decomposition process. Both tetraalkylammonium and 1,4-dimethylpyridinium salts of $[Bi(dmit)_2]^-$ decompose with a F_1 mechanism, which indicates that the first step of thermal decomposition of these systems is strongly influenced by the anion reaction. This statement does not hold for the [Q]Br salts, which exhibit different thermal decomposition mechanisms depending on [Q]. The influence of the cation on the decomposition of $[Q][Bi(dmit)_2]$ is not evident, since the mechanisms are most probably associated to both molecular and solid-state structures.

The thermodynamic parameters obtained for each decomposition reaction reflect the mechanism associated as well as the specific characteristics of the systems under study. In general, the $\Delta G^{\#}$ (positive) values are found between 111.70 and 133.41 kJ mol^{-1}, while $\Delta H^{\#}$ (also positive) values exhibit a broader range, between 114.43 and 285.47 kJ mol^{-1}. In contrast, the $\Delta S^{\#}$ values seem to be more influenced by the molecular structure, varying from −21.12 to 338.98 J mol^{-1}.

Acknowledgments Authors would like to thank FAPERJ and CNPq for financial support and research fellowships.

References

1. Cassoux P. Molecular (super)conductors derived from bis-dithiolate metal complexes. Coord Chem Rev. 1999;185:213–32.
2. Yamochi H, Koshihara S. Organic metal (EDO-TTF)$_2$PF$_6$ with multi-instability. Sci Technol Adv Mater. 2009;10:024305.
3. Kobayashi A, Kim H, Sasaki Y, Kato R, Kobayashi H, Moriyama S, Nishio Y, Kajita K, Sasaki W. The 1st molecular superconductor based on pi-acceptor molecules and closed-shell cations, $[(CH_3)_4N][Ni(dmit)_2]_2$, low-temperature X-ray studies and superconducting transition. Chem Lett. 1987;9:1819–22.
4. Ganis P, Marton D, Spencer GM, Wardell JL, Wardell SMSV. The molecular and crystal structure of tetraphenylphosphonium antimony(III) bis-dmit. A comparison with similar complexes. Inorg Chim Acta. 2000;308:139–42.
5. Bryce MR. Conductive charge-transfer complexes. In: Petty MC, Bryce MR, Bloor D, editors. An introduction to molecular electronics. New York: Oxford University Press; 1995. p. 168–83.
6. Bonneval BG, Ching KIMC, Alary F, Bui TT, Valade L. Neutral d(8) metal bis-dithiolene complexes: synthesis, electronic properties and applications. Coord Chem Rev. 2010;254:1457–67.
7. Russell DK. Gas-phase pyrolysis mechanisms in organometallic CVD. Chem Vap Depos. 1996;2:223.
8. DeArmond MK, Fried GA. Langmuir-Blodgett films of transition metal complexes. Progr Inorg Chem. 1997;44:97–142.
9. Pereira RP, Wardell JL, Rocco AM. Electrosynthesis and characterisation of polypyrrole doped with $[Bi(dmit)_2]^-$. Synth Met. 2005;150:21–6.
10. Harrison WTA, Howie AR, Wardell JL, Wardell SMSV, Comerlato NM, Costa LAS, Silvino AC, Oliveira AI, Silva RM. Crystal structures of three [bis(1, 3-dithiole-2-thione-4, 5-dithiolato)zincate]$^{2-}$ salts: $[Q]_2[Zn(dmit)_2]$ (Q = 1, 4-Me-2-pyridinium or NEt_4) and $[PPh_4]_2[Zn(dmit)_2]$.DMSO. Comparison

of the dianion packing arrangements in $[Q]_2[Zn(dmit)_2]$. Polyhedron. 2000;19:821–7.
11. Rocco AM, Pereira RP, Bonapace JAP, Comerlato NM, Wardell JL, Milne BF, Wardell SMSV. A theoretical study of tetrabutylammonium [bis(1, 3-dithiole-2-thione-4, 5-dithiolato)bismuthate], $[NBu_4][Bi(dmit)_2]$: infrared spectrum in the solid state and solvation effects on the molecular geometry. Inorg Chim Acta. 2004;357:1047–53.
12. Comerlato NM, Costa LAS, Howie RA, Pereira RP, Rocco AM, Silvino AC, Wardell JL, Wardell SMSV. Synthesis and properties of bis(1, 3-dithiole-2-thione-4, 5-dithiolato)bismuthate(1−) salts $[Q][Bi(dmit)_2]$. Crystal structure of $[AsPh_4][Bi(dmit)_2].½DMSO$: comparison of the solid state structures of $[Q][Bi(dmit)_2]$ and $[Q][Sb(dmit)_2]$. Polyhedron. 2001;20:415–21.
13. Sharp JH, Brindley GW, Achar BNN. Numerical data for some commonly used solid state reaction equations. J Am Ceram Soc. 1066;49:379.
14. MacCallum JR, Tanner J. Kinetics of thermogravimetry. Eur Polym J. 1970;6:1033–9.
15. Horowitz HH, Metzger G. A new analysis of thermogravimetric traces. Anal Chem. 1963;35:1464–8.
16. Coats AW, Redfern PJ. Kinetic parameters from thermogravimetric data. Nature. 1964;201:68–9.
17. Ozawa T. A new method of analyzing thermogravimetric data. Bull Chem Soc Jpn. 1965;38:1881–6.
18. Soliman AA, Ali SA, Khalil MMH, Ramadan RM. Thermal studies of chromium, molybdenum and ruthenium complexes of chloranilic acid. Thermochim Acta. 2000;359:37–42.
19. Mahfouz RM, Al-Farhan KA, Hassen GY, Al-Wassil AI, Alshehri SM, Al-Wallan AA. Preparation and characterization of new In(III), Re(III), and Re(V) complexes with thenoyltrifluoroacetone and some bidentate heterocyclic ligands. Synth React Inorg Met-Org Chem. 2002;32:489–508.
20. Melo DMA, Borges FMM, Lima FJS, Scatena H, Zinner LB, Fernandes VJ, Souza WSC, Silva ZR. Kinetic study of thermal decomposition of the dmit complex of cobalt. J Therm Anal Calorim. 1999;56:805–10.
21. El-Ayaan U, Youssef MM, Al-Shihry S. Mn(II), Co(II), Zn(II), Fe(III) and U (VI) complexes of 2-acetylpyridine N-4-(2-pyridyl) thiosemicarbazone (HAPT); structural, spectroscopic and biological studies. J Mol Struct. 2009;936:213–9.
22. Doğan F, Kaya İ, Bilici A, Saçak M. Thermal decomposition kinetics of azomethine oligomer and its some metal complexes. J Appl Polym Sci. 2010;118:547–56.
23. Sánchez G, García J, Pérez J, García G, Lopez G. Synthesis and thermal behaviour of pentamethylcyclopentadienylrhodium(III) complexes with anilines. Thermochim Acta. 1997;307:127–34.
24. Dollimore D, Tong P, Alexander KS. The kinetic interpretation of the decomposition of calcium carbonate by use of relationships other than the Arrhenius equation. Thermochim Acta. 1996;282/283:13–27.
25. Heda PK, Dollimore D, Alexander KS, Chen D, Law E, Bicknell P. Method of assessing solid-state reactivity illustrated by thermal-decomposition experiments on sodium-bicarbonate. Thermochim Acta. 1995;255:255–72.
26. Diefallah EHM, Obaid AY, Qusti AH, El-Bellihi AA, Wahab MA, Moustafa MM. Gamma irradiation effects on the kinetics of the non-isothermal decomposition of manganese acetate tetrahydrate. Thermochim Acta. 1996;274:165–72.
27. Yang LR, Shao CY, Wang ZL, Liu JT, Zhou LF. Crystal structure and thermodecomposition kinetics of Mn(II) complex with 1-phenyl-3-methyl-4-benzoyl-5-pyrazolone. J Chem Crystallogr. 2010;40:58–63.
28. Boonchom B. Kinetic and thermodynamic studies of $MgHPO_4 \cdot 3H_2O$ by non-isothermal decomposition data. J Therm Anal Calorim. 2009;98:863–71.